Electric Field Reconstruction of Antenna inside Phantom for Non-invasive SAR Measurement

Rasyidah Hanan Binti Mohd Baharin[1*], Toru Uno[1], Takuji Arima[1] and Shuntaro Omi[2]
[1]Department of Electronic and Information Engineering, Tokyo University of Agriculture and Technology, Japan
[2]Applied Electromagnetic Research Institute, National Institute of Information and Communications Technology, Japan
[*]email: rh.baharin@gmail.com

***Abstract* – This paper studies electric field reconstruction for antenna inside phantom. The application is aimed for non-invasive SAR measurement of in-body antenna. The method relates electromagnetic currents on the surface enclosing the test subject (antenna and phantom combination) to the scattered external field received by probe. From the surface currents, we were able to reconstruct the internal electric field of phantom with known permittivity, $\varepsilon_r = 45$. It is shown that we can obtain good result in lossless sphere case.**

***Keywords* — Electromagnetic fields, antenna measurements, inverse problem, specific absorption rate**

I. INTRODUCTION

In recent years, the advancement of wireless biomedical telemetry devices is rapidly growing. There are various ingestible and implantable antenna deployed inside of human body such as wireless capsule endoscopy which is used to monitor the gastrointestinal system [1]. As a result, specific absorption rate (SAR) measurement plays a pivotal role to ensure these devices are working within the safety limits determined by the authority.

SAR is defined by the amount of electromagnetic (EM) energy absorption per unit mass, where SAR = $\sigma|\mathbf{E}|^2/\rho$. Hence, at the selected measurement point, SAR can be obtained if the electric field distribution ($\mathbf{E}$) is known. It is widely known that the conventional SAR measurement involves probe insertion into liquid phantom illuminated by the antenna [2]. With this method, SAR value can be obtained accurately due to probe scanning in in three dimensions. The apparent drawback is the invasive nature and substantial calculation time due to volumetric data. Therefore, a non-invasive SAR measurement method that utilizes surface current data is ideal. Furthermore, due to the probe measurement taking place outside of phantom, a more stable solid phantom can be used.

In this paper, we aim to reconstruct the internal field of antenna inside of phantom from external field measurement data. We base our study by referring to the method in [3], where the internal field of phantom (illuminated by an external antenna) was reconstructed with probe correction applied on the receiving terminal. In our case, the antenna is inside of the phantom and radiates as a single source. The reconstruction method is based on surface equivalent theorem whereby the EM surface currents of the phantom are related to the arbitrary measurement's surface by considering appropriate boundary conditions. Then, the geometry is discretized by using Poggio-Miller-Chan-Harrington-Wu (PMCHW) formulation, and further reduced into matrix form using Rao-Wilton-Glisson (RWG) basis functions for EM currents [4]. By solving the discretized functions, we can reconstruct the electric field.

II. SOURCE RECONSTRUCTION

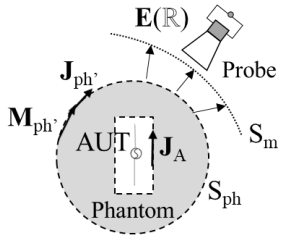

Fig. 1. Phantom with AUT embedded inside.

The dosimetry problem under consideration is shown in Fig. 1. An antenna under test (AUT) is in the center of a phantom. This situation imitates an implantable antenna or ingestible antenna inside of a human body. $\mathbf{J}_{ph'}$ and $\mathbf{M}_{ph'}$ is the equivalent EM surface currents on the phantom's surface, S_{ph}. The (') denotes that the currents are a combination of AUT's electric current $\mathbf{J}_A$ and the true $\mathbf{J}_{ph}$ and $\mathbf{M}_{ph}$. Here, we consider a single equation formulation (SEqF) where only the electric current source is considered. The radiated field from scattering observed by the probe is given as (1). The first term on the right-hand side is the electric field from electric current, while the second term is from magnetic current. From there, $\mathbf{E}$-field at any points inside the phantom then is given as (2).

$$\mathbf{E}(\mathbb{R}) = -\eta_0 \mathscr{L}_{k0}(\mathbf{J}_{ph'}; \mathbb{R}) + \mathscr{M}_{k0}(\mathbf{M}_{ph'}; \mathbb{R}) \quad (1)$$

$$\mathbf{E}(\mathbb{R}) = \mathscr{L}_{k1}(\eta_1 \mathbf{J}_{ph'}; \mathbb{R}) - \mathscr{M}_{k1}(\mathbf{M}_{ph'}; \mathbb{R}) \quad (2)$$

The impedances and wavenumbers η_0/k_0 and η_1/k_1 correspond to that of free space and phantom, respectively. Meanwhile, $\mathscr{L}$ and $\mathscr{M}$ are the integral operators for electric currents (3) and magnetic currents (4). G indicates the scalar Green's function of the given wavenumber k.

$$\mathscr{L}^k(\mathbf{X}; \mathbb{R}) = jk \iint_S \left[\frac{1}{k^2} \nabla G^k(\mathbb{R}, \mathbb{R}') \nabla' \cdot \mathrm{X}(\mathbb{R}') + G(\mathbb{R}, \mathbb{R}') \mathrm{X}(\mathbb{R}') \right] dS' \quad (3)$$

$$\mathcal{M}^{k}(\mathbf{X};\mathbb{R}) = \oiint_{S} \nabla G^{k}(\mathbb{R},\mathbb{R}') \times \mathrm{X}(\mathbb{R}')\, dS' \tag{4}$$

Then, we solve the relation in (1) where $\mathbf{J}_{ph'}$ and $\mathbf{M}_{ph'}$ are represented by PMCHW as in (5). Equation (5) relates $\mathbf{J}_A$ to $\mathbf{J}_{ph'}$ and $\mathbf{M}_{ph'}$. The subscript P and A represents phantom and AUT, respectively.

$$\begin{bmatrix}\mathbf{J}_{ph\prime}\\ \mathbf{M}_{ph\prime}\end{bmatrix} = \left(\hat{n}\times\begin{bmatrix}-\mathcal{L}_{PP}^{k_0}-\mathcal{L}_{PP}^{k_1} & \mathcal{K}_{PP}^{k_0}+\mathcal{K}_{PP}^{k_1}\\ \mathcal{K}_{PP}^{k_0}+\mathcal{K}_{PP}^{k_1} & \mathcal{L}_{PP}^{k_0}+\mathcal{L}_{PP}^{k_1}\end{bmatrix}^{-1}\right) \begin{bmatrix}-\hat{n}\times\eta_0\mathcal{L}_{PA}^{k_1}\\ \hat{n}\times\mathcal{K}_{PA}^{k_1}\end{bmatrix}[\mathbf{J}_A] \tag{5}$$

III. SIMULATION MODEL

We tested the method numerically with a spherical phantom. The measurement surface is assumed on spherical coordinates, taken from a commercial simulator. In this simulation, only the phi (ϕ) component of the **E**-field is used for the reconstruction. The simulation parameters are summarized in Table I and the reconstruction surface meshed into 3616 triangles is shown in Fig. 2.

TABLE I SIMULATION PARAMETERS

Parameters	Settings	
Calculation	Method of Moments (MoM)	
Frequency	f = 2.5GHz	
Dielectric (Phantom)	Sphere, radius = 5cm	ε_r = 45; σ = 0
AUT (Dipole)	PEC; Length = 0.045cm (~0.25λ_{ph})	
Probe sampling	Distance = 60 cm; Interval, $\Delta\varphi = \Delta\theta = 5^{o}$	

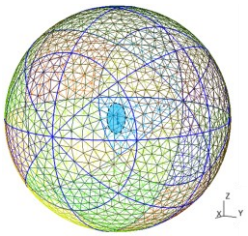

Fig. 2. Reconstruction surface of AUT in phantom. Circled is a thin cylinder as the boundary of AUT [5].

The boundary of the phantom is selected to be the same as that of the dimension of the sphere and AUT. As for the dipole's dimension, it must be minimized adequately in proportion to the wavelength of the phantom, λ_{ph}. Through trial and error, we have selected a dipole of length 0.045 cm, assuming there is no air gap between the boundary of phantom and dipole.

IV. RESULTS

The reconstruction results of surface currents (**J**) are shown in Fig. 3, while **E**-field distribution in Fig. 4. On the left side is from reconstruction and on the right side is the reference calculated by direct solution. In both cases, the distribution pattern and magnitude of the current, **J** and **E**-field is satisfactory. In Fig. 4 (left), the reconstructed **E**-field in antenna proximity is less accurate compared to reference. This is due to nature of MoM-based solver in calculating currents relatively close to wire.

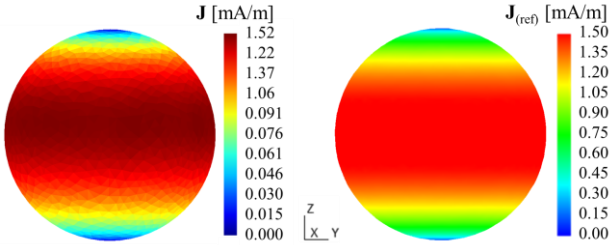

Fig. 3. Surface current (**J**) of phantom.

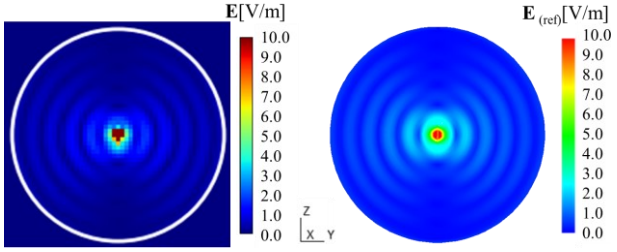

Fig. 4. Internal electric field (**E**) of phantom.

V. CONCLUSION

In this paper, we proposed a method for reconstruction of electric field for a phantom with embedded antenna. With this method, the internal electric field distribution of a lossless phantom at high permittivity can be predicted from the surface field measurement of the probe. However, the calculation involves a lossless phantom (perfect dielectric) and is not so practical for dosimetry, as it is nearly impossible for the human tissue to be lossless. For this reason, lossy tissue will be studied in future tests.

REFERENCES

[1] K. S. Nikita, Handbook of Biomedical Telemetry, New Jersey: John Wiley & Sons, 2014, p. 2.

[2] H. Arai, Measurement of Mobile Antenna Systems, Massachusetts: Artech House, 2013, pp. 119-120.

[3] S. Omi, T. Uno, T. Arima, and J. Wiart, "Reconstruction of Internal Field of Dielectric Objects for Noninvasive SAR Measurement Using Boundary Integral Equation," *IEEE Transactions on Electromagnetic Compatibility*, Volume 61, Issue 1, pp. 48-56, 2019.

[4] R. Mitharwal and F. P. Andriulli, "A regularised boundary element formulation for contactless SAR evaluations within homogeneous and inhomogeneous head phantoms," *Comptes Rendus Physique*, vol. 16, no. 9, pp. 776-788, 2015.

[5] C. Geuzaine and J.-F. Remacle. Gmsh: a three-dimensional finite element mesh generator with built-in pre- and post-processing facilities. *International Journal for Numerical Methods in Engineering*, 79(11), pp. 1309-1331, 2009.